Available online at www.sciencedirect.com
SCIENCE DIRECT
Biochimica et Biophysica Acta 1717 (2005) 1 – 10
BIOCHIMICA ET BIOPHYSICA ACTA
BBA
http://www.elsevier.com/locate/bba

Type 1 ryanodine receptor in cardiac mitochondria: Transducer of excitation–metabolism coupling

Gisela Beutner [a], Virendra K. Sharma [a], Lin Lin [a], Shin-Young Ryu [a], Robert T. Dirksen [a], Shey-Shing Sheu [a,b,*]

[a] *Department of Pharmacology and Physiology, Box 711, University of Rochester, School of Medicine and Dentistry, 601 Elmwood Avenue, Rochester, NY 14642, USA*
[b] *Departments of Pharmacology and Physiology, Anesthesiology, Medicine and the Mitochondrial Research Interest Group, University of Rochester, School of Medicine and Dentistry, 601 Elmwood Avenue, Rochester, NY 14642, USA*

Received 25 June 2004; received in revised form 21 September 2005; accepted 21 September 2005
Available online 11 October 2005

Abstract

Mitochondria in a variety of cell types respond to physiological Ca^{2+} oscillations in the cytosol dynamically with Ca^{2+} uptakes. In heart cells, mitochondrial Ca^{2+} uptakes occur by a ruthenium red-sensitive Ca^{2+} uniporter (CaUP), a rapid mode of Ca^{2+} uptake (RaM) and a ryanodine receptor (RyR) localized in the inner mitochondrial membrane (IMM). Three subtypes of RyRs have been described and cloned, however, the subtype identity of the mitochondrial ryanodine receptor (mRyR) is unknown. Using subtype specific antibodies, we characterized the mRyR in the IMM from rat heart as RyR1. These results are substantiated by the absence of RyR protein in heart mitochondria from RyR1 knockout mice. The bell-shape Ca^{2+}-dependent [^{3}H]ryanodine binding curve and its modulation by caffeine and adenylylmethylenediphosphonate (AMPPCP) give further evidence that mRyR functions pharmacologically like RyR1. Ryanodine prevents mitochondrial Ca^{2+} uptake induced by raising extramitochondrial Ca^{2+} to 10 μM. Similarly, ryanodine inhibits oxidative phosphorylation stimulated by 10 μM extramitochondrial Ca^{2+}. In summary, our results show that the mRyR in cardiac muscle has similar biochemical and pharmacological properties to the RyR1 in the sarcoplasmic reticulum (SR) of skeletal muscle. These results could also suggest an efficient mechanism by which mitochondria sequesters Ca^{2+} via mRyR during excitation–contraction coupling to stimulate oxidative phosphorylation for ATP production to meet metabolic demands. Thus, the mRyR functions as a transducer for excitation–metabolism coupling.

Keywords: Heart; Mitochondria; Mitochondrial ryanodine receptor; Calcium; Oxygen consumption

1. Introduction

Mitochondrial Ca^{2+} uptake plays an essential role in the regulation of numerous cellular processes including energy metabolism and cytosolic Ca^{2+} homeostasis [1–4]. Dysfunction of these Ca^{2+}-regulated processes has been implicated in the development of diseases such as cardiomyopathy [5], diabetes [6], and neurodegeneration [7]. Consequently, mitochondrial Ca^{2+} uptake mechanisms, generally named as Ca^{2+} uniporters (CaUP), have been studied extensively (for review see [8]).

Although recent advances of patch-clamp techniques have contributed to the pharmacological and biophysical characterization of Ca^{2+} activated channels in the IMM [9–11], these efforts have yielded little information regarding the molecular identity of these mitochondrial Ca^{2+} transport mechanisms. Presently, the only known molecular identity of a mitochondrial Ca^{2+} transporter is our recent discovery of a mRyR in the IMM of rat heart, which mediates a fast,

Abbreviations: Ca^{2+}, calcium; CaUP, mitochondrial calcium uniporter; RR, ruthenium red; SR, sarcoplasmic reticulum; RyR, ryanodine receptor; SR-RyR, sarcoplasmic RyR; mRyR, mitochondrial RyR; SERCA, sarco- and endoplasmic reticulum Ca^{2+} ATPase; IMM, inner mitochondrial membrane; VDAC, voltage gated anion channel; AMPPCP, adenylylmethylenedi-phosphonate; RCI, respiratory control index

* Corresponding author. Department of Pharmacology and Physiology, Box 711, University of Rochester, School of Medicine and Dentistry, 601 Elmwood Avenue, Rochester, NY 14642, USA. Tel.: +1 585 275 3381; fax: +1 585 273 2652.
E-mail address: sheyshing_sheu@urmc.rochester.edu (S.-S. Sheu).

0005-2736/$ - see front matter © 2005 Elsevier B.V. All rights reserved.
doi:10.1016/j.bbamem.2005.09.016

ryanodine- and dantrolene-sensitive Ca^{2+} uptake [12]. Interestingly, the pharmacological characteristics of the mRyR, such as a bell-shaped Ca^{2+} dependency of [^{3}H]ryanodine binding, the inhibition of [^{3}H]ryanodine binding in the presence of Mg^{2+} (IC_{50}=0.29 mM), ruthenium red (RR, IC_{50}=74 nM), and dantrolene, are reminiscent of the skeletal muscle RyR in the sarcoplasmic reticulum (SR), RyR1 [12–15]. Another intriguing property of the mRyR is its ability for fast Ca^{2+} transport. In response to extramitochondrial Ca^{2+} pulses, Ca^{2+} uptake by the mRyR peaks within the shortest sampling interval of one image frame that was used (250 ms, [12]). This observed fast Ca^{2+} uptake kinetics is similar to that of mitochondrial ATP production in response to extramitochondrial Ca^{2+} pulses, which occur within 150 ms [16]. Therefore, an attractive hypothesis is that the mRyR serves as a conduit between extramitochondrial Ca^{2+} pulses and intramitochondrial ATP generation.

The aims of this study are to test the hypothesis that (1) the mRyR is comprised of the type 1 RyR isoform, and (2) the mRyR is an important mitochondrial Ca^{2+} uptake mechanism for Ca^{2+} stimulated oxygen (O_2) consumption. Using immunological, pharmacological, and physiological methods, we show here that the cardiac mRyR behaves like the skeletal muscle RyR1. In addition, Ca^{2+} uptake through the mRyR activates mitochondrial O_2 consumption, indicative for mitochondrial ATP generation. These results suggest that, in addition to the well-described role of releasing Ca^{2+} from the SR of skeletal muscle for generating contraction, RyR1 channels serve as a critical Ca^{2+} uptake mechanism in cardiac mitochondria for increasing ATP production.

2. Methods

2.1. Material

Ryanodine was purchased from Calbiochem (San Diego, CA) and [^{3}H]ryanodine from Amersham (Piscataway, NJ). Antibodies against the RyR were obtained from the following sources: RyR1: XA 7B6, Upstate Biotechnology (Charlottesville, VA); RyR2: Clone C3-33 from RBI/Sigma (St. Louis, MO); RyR1-3: RyR N19 from Santa Cruz (Santa Cruz CA), RyR3: a generous gift from Dr. Gerhard Meissner, University of North Carolina. Antibodies against VDAC and the sarco- and endoplasmic reticulum ATPase (SERCA) were obtained from Calbiochem (San Diego, CA), and Santa Cruz (Santa Cruz, CA), respectively. Protease inhibitor Complete was purchased from Roche Applied Science (Indianapolis, IN). All other chemicals were purchased from Sigma unless noted otherwise.

2.2. Methods

All procedures for animal use were in strict accordance with *the NIH Guide for the Care and Use* of Laboratory Animals, and were approved by the University Committee on Animal Resources.

2.2.1. RT-PCR

For RT-PCR, the total RNA of 1 rat heart or acutely dissociated single cardiomyocytes from 1 rat heart was extracted using the RNeasy Mini Kit from Qiagen. For subsequent cDNA synthesis the Superscript™ one-step RT-PCR with Platinum Taq (Invitrogen, Carlsbad, CA) was used. RT-PCR was performed according to the instructions given by the supplier. The primers summarized in Table 1 were used to specifically amplify RNA for RyR1, RyR2, and RyR3.

Table 1
Primers used for RyR subtype-specific RNA amplification

Protein	Primer sequence	Base pairs	Reference
RyR1	5′-GGTGGCCTTCAACTTCTTC-3′ (forward) 5′-ACTTGCTCTTGTTGGTCTCCG-3′ (reverse)	293	[55]
RyR2	5′-GAATCAGTCAGTTACTGGGCATGG-3′ (forward) 5′-CTGGTCTCTGAGTTCTCCAAAAGC-3′ (reverse)	635	[31]
RyR3	5′-AGAAGAGCCCAAAGCAGAGG-3′ (forward) 5′-GGAGGVVAACGGTCAGA-3′ (reverse)	505	[30]

2.2.2. Isolation of rat heart mitochondria and SR microsomes

Mitochondria were isolated in ice-cold mannitol/sucrose-buffer (M/S buffer; containing in mM: 225 mannitol, 10 sucrose, 0.5 EGTA, 10 HEPES, pH 7.4) by differential centrifugation at 500 and 12,000 g, followed by a purification on a Percoll gradient as described earlier [12,17].

The post-mitochondrial supernatant, obtained after the first centrifugation at 12,000 g, which contains beside cytosolic components SR (heart) and ER (brain) microsomes, was used to enrich RyR-containing microsomes by centrifugation for 60 min at 150,000×g. The resulting sediment containing RyR-microsomes was resuspended in a small volume of M/S buffer supplemented with protease inhibitor. Note that this post-mitochondrial supernatant was obtained after gentle disrupting the cell membranes of cardiac or brain tissue with a Teflon-coated potter. As a consequence, the quantity of RyR-containing microsomes, specifically from cardiac SR is relatively low (see Fig. 1B, RyR2 lane b) compared to highly optimized protocols published recently [13,18]. Preparations using the latter protocols result normally in much stronger signals for RyR2 protein (data not shown).

2.2.3. Preparation of mitochondrial subfractions

IMM vesicles were prepared from isolated rat heart mitochondria by sucrose-density centrifugation as described previously [12,19]. For all experiments described here, only such IMM preparations that exhibited a high succinate dehydrogenase activity (an enzyme, which is found only in the IMM), but tested negative for SERCA and VDAC (indicative for proteins of the SR and the outer mitochondrial membrane, respectively) were used (Fig. 1B SERCA and Fig. 1D).

2.2.4. Isolation of heart mitochondria from neonatal mice

Dyspedic RyR1 knockout mice contain 2 disrupted alleles for RyR1 resulting in a lethal birth defect [20,21]. These mice die immediately after they are born. For this reason, the tissue homogenates or mitochondria from RyR1 knockout mice were obtained immediately after these mice were born. In addition, all experiments were repeated with age-matched surviving control mice, which were either +/+ or +/− for RyR1, to compensate for possible developmental differences between the neonatal mice and adult animals.

The hearts from 2 to 6 newborn RyR1 knockout mice or phenotypically normal littermate were homogenized in 0.5 ml M/S buffer supplemented with protease inhibitor. After centrifugation for 10 min at 500×g in a tabletop centrifuge at 4 °C to remove blood cells, plasma membrane fragments and nuclei, the supernatant was centrifuged for 5 min at 15,000×g. The mitochondria containing sediment was resuspended in M/S-buffer, centrifuged again for 5 min at 15,000×g, and then resuspended in 20–40 μl M/S buffer. A sample of isolated heart mitochondria from one RyR1 knockout mouse yields on average in 18±3 μg protein ($n \geq 75$).

2.2.5. Skeletal muscle microsomes

Skeletal muscle microsomes were obtained from mostly white muscle of the hind legs of 2 rats according to a modified protocol published recently [18]. Connective tissue and red appearing muscle tissue were removed by

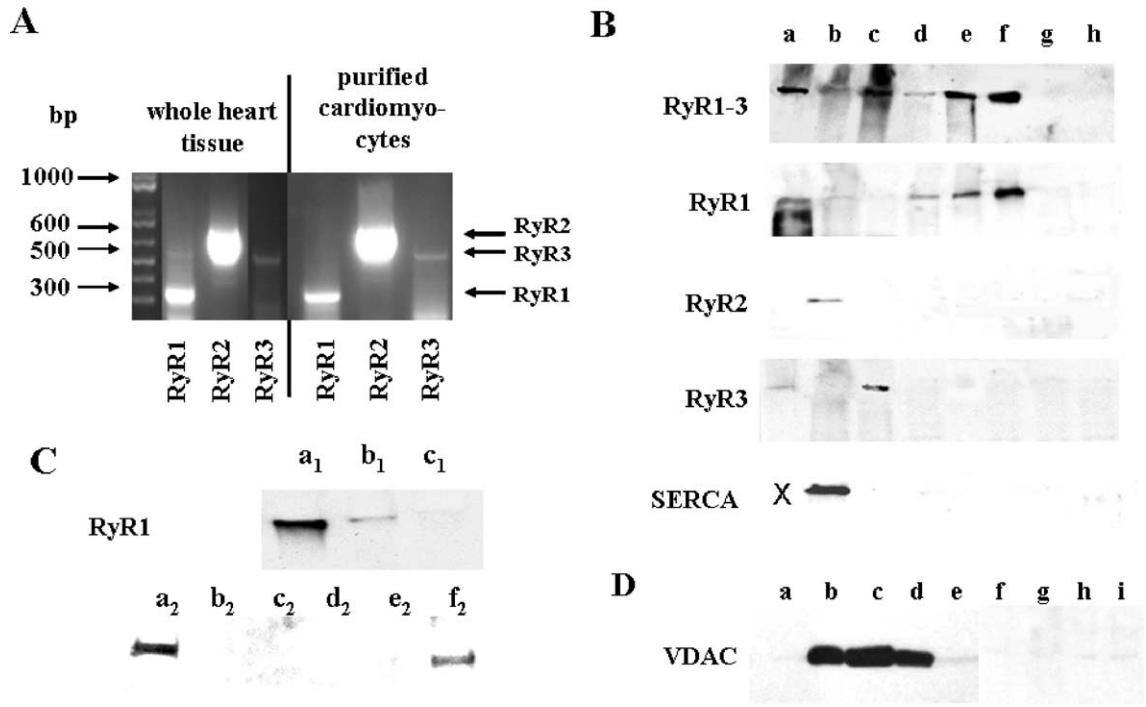

Fig. 1. RT-PCR and Western blot analysis of RyR1, RyR2, and RyR3 in rat and mouse hearts. (A) RT-PCR of total RNA from 1 rat heart (left) and acutely dissociated single cardiomyocytes (right) from 1 rat heart demonstrate the message for all 3 RyR subtypes. (B) Western blot analysis with RyR subtype-specific antibodies. Per lane 60 μg of protein was used. Probes in lanes a–e are obtained from adult rats while probes in lane f were from adult mice and RyR1 knockout mice (g–h). To minimize variations due to different preparations and antibodies used at different dates of experiments, all blots in B were done concurrently. Moreover, all blots in lanes a–f were done with aliquots from the same preparation isolated either from skeletal muscles, heart, or brain. Finally, the samples used for blotting in lanes b, d, and e were all obtained from the same hearts. a: Skeletal muscle SR, b: cardiac SR microsomes, c: ER containing cytosol from brain, d: heart mitochondria, e: IMM from heart mitochondria, f: mitochondria from adult mouse, g and h: mitochondria from RyR1 knockout mice. SERCA: Isolated mitochondria from rat heart or the IMM fractions are free of detectable amounts of SERCA. Note that the detection of SERCA begins in lane b (cardiac SR microsomes). The here used antibody will detect SERCA protein in the heart or the skeletal muscle but not in the brain. (C) RyR1 protein is detected in heart mitochondria from adult (lanes a_1 and a_2) and neonatal control mice (lane b_1 and lane f_2), but not in neonatal RyR1 knockout mice (lane c1 and the lanes b_2–e_2). Per lane, 60 μg of protein was used. Mitochondrial samples from neonatal control mice contained hearts from both homozygous and heterozygous normal mice. (D) IMM preparations from rat heart mitochondria are virtually free of VDAC. The samples in lanes a–e were obtained from the same hearts as those samples used for the lanes b, d and e in Fig. 1B. a: cardiac SR microsomes (50 μg protein), b: heart mitochondria (20 μg protein), c: outer mitochondrial membrane (20 μg protein), d: contacts between outer and inner mitochondrial membrane (50 μg protein), e: IMM (50 μg protein), f–i: IMM fractions from 4 different preparations (50 μg protein).

dissecting the legs on a glass tray placed on packed ice. The dissected tissue was minced in ice-cold isolation buffer (300 mM sucrose, 5 mM imidazol pH 7.4, protease inhibitor cocktail Complete) and then homogenized (2 times for 30 s at half-maximal speed) with a Polytron homogenizer. The homogenate was centrifuged for 10 min at 500×*g*. The supernatant was stored on ice and the sediment was homogenized and centrifuged again as before. Skeletal muscle microsomes were obtained from both supernatants by centrifugation at 30,000×*g* for 20 min.

For [^{3}H]ryanodine binding experiments the sediment was resuspended in a small volume of isolation buffer. For Western blots, the RyR-containing microsomes were further purified on a discontinuous sucrose gradient (45, 38, 32, and 27% sucrose) and centrifuged for at least 14 h at 72,000×*g* [18]. The strongest RyR-signal was obtained from the fractions at the interface between 32/38 and 38/45% sucrose. These fractions were collected, diluted with isolation buffer and centrifuged for 90 min at 100,000×*g* in a Ti60 rotor. The sediment was resuspended in a small volume of isolation buffer.

2.2.6. Denaturing SDS gel electrophoresis

For the immunological detection of the RyR and SERCA, 60 μg protein was loaded on a 5% SDS-page. To transfer RyR or SERCA protein, the separated proteins were transferred onto a nitrocellulose membrane for 18 h at 35 V or 25 V, respectively. For the immunological detection of VDAC, 20–50 μg protein was loaded onto a 12% SDS page and transferred for 50 min at 90 V onto a nitrocellulose membrane. For some experiments, pre-made gradient gels from Biorad (4–15% acrylamide/bisacrylamide for proteins bigger than 60 kDa and 10 to 20% acrylamide/bisacrylamide for proteins smaller than 60 kDa) were used. Western blots were performed using the ECL kit (Amersham, Piscataway, NJ) with a horseradish peroxidase-conjugated secondary antibody. Equal protein loading and protein transfer was ensured by the intensity of the Ponceau Red staining of the nitrocellulose membrane (not shown).

To obtain sufficient amounts of protein for the immunological detection of RyR protein from neonatal samples, isolated mitochondria from several preparations were pooled. To simplify analysis, each of these pooled samples was counted as one preparation.

2.2.7. [^{3}H]ryanodine binding

For binding assays, 100 μg mitochondrial proteins were incubated with different concentrations of [^{3}H]ryanodine in 0.5 ml binding buffer (in mM: 170 KCl, 10 MOPS, pH 7.0) and the indicated Ca^{2+} concentration for 16 h at 25 °C as described before [12]. For the determination of non-specific binding, because ryanodine only binds to the open state of RyR, 6 mM EGTA was added to the Ca^{2+}-free binding buffer to lock RyR in the close state completely. Calcium standard solutions were prepared with 1 mM EGTA in ryanodine binding buffer by adding appropriate amounts of a 100 mM $CaCl_2$ solution. The free Ca^{2+} concentration was then determined according to [22]. At the end of the incubation time, the reaction mixture was filtered under reduced pressure through glass fiber filters (Whatman GF/B, Maidstone, UK) and washed with ice-cold buffer three times. The radioactivity in the dried membranes was counted with a liquid scintillation counter using a toluene-based scintillator.

2.2.8. Oxygen consumption assays

O_2 consumption of isolated mitochondria from rat hearts (1 mg protein) or cardiac tissue homogenates obtained from neonatal mouse hearts (0.3 mg protein) was measured with a Clark-electrode (Hansatech, Norfolk, UK). Samples were either directly diluted in M/S buffer supplemented with 0.01 mM EGTA (to chelate Ca^{2+} impurities in the water), 1 mM Mg^{2+} and 5 mM potassium phosphate or after the incubation with 20 μM ryanodine. Incubation with 20 μM ryanodine (15 min at room temperature) was done in M/S buffer before the addition of EGTA, Mg^{2+} and potassium phosphate to ensure high affinity ryanodine binding. Oxidative phosphorylation was stimulated with 10 μM Ca^{2+} in the presence of 5 mM malate and 5 mM glutamate as substrate. While Ca^{2+} can uncouple oxidative phosphorylation, low concentrations of this cation have been reported to specifically stimulate the Ca^{2+}-regulated dehydrogenases of the TCA cycle [23]. The respiratory control index (RCI [24]) indicates the ability of isolated mitochondria to use ADP for ATP generation in the presence of a substrate. To calculate the RCI, defined as the ratio of maximal respiration over substrate-induced respiration, the measured maximal O_2 consumption in presence of 1 mM ADP was divided by the substrate-mediated O_2 consumption (i.e., in the presence of 5 mM succinate or 5 mM malate and 5 mM glutamate).

2.2.9. Measurements of mitochondrial Ca^{2+} influx with Fura-FF

Isolated heart mitochondria from adult rats were diluted in modified M/S buffer (in mM: 120 KCl, 65 mannitol, 30 sucrose, 10 succinate, 5 Na_2HPO_4/NaH_2PO_4, 10 HEPES, pH 7.2) to a final protein concentration of approximately 5 mg/ml. Mitochondria were then loaded with the low affinity Ca^{2+} indicator Fura-FF (5 μM) in the presence of 0.02% pluronic acid (Gibco, Carlsbad, CA) for 15 min at room temperature. After washing the mitochondria 3 times with M/S buffer, supplemented with 10 μM EGTA, mitochondria were kept for 15 min at room temperature to allow complete de-esteration of the fluorescence dye. The changes of mitochondrial Ca^{2+} net uptake were monitored with a Perkin-Elmer LS-5 fluorescence spectrophotometer. The excitation wavelength was 380 nm and the emission wavelength was 510 nm. Under these experimental conditions, Ca^{2+} influx causes a decrease in the fluorescence (F) signal, which was normalized to the baseline fluorescence (F_o). Results are expressed as F_o/F, so that values greater than 1 reflect an increased Ca^{2+} net influx into the mitochondria.

3. Results

3.1. RT-PCR indicates the presence of mRNA for all 3 RyR subtypes in muscle cells from rat heart

Three different RyR isoforms (RyR1, RyR2, and RyR3) have been cloned and are pharmacologically described (for reviews see [25,26]). Although the expression of the RyR subtypes is somewhat tissue specific, with RyR1 being the major isoform in skeletal muscle, RyR2 in cardiac and smooth muscle, and RyR3 in the brain, several tissues express more than one RyR subtype. For example, RyR1 and RyR3 are expressed in the diaphragm, and during early developmental stages both are expressed throughout the skeletal muscle [27]. RT-PCR with RNA extracts from total rat heart tissue and purified individual rat adult cardiomyocytes shows the message of all three RyR-subtypes (Fig. 1A). The strongest signal was obtained for RyR2, and much weaker signals were obtained for RyR1 and RyR3 ($n=3$). The signals for RyR1 and RyR3 do not arise from fibroblasts, smooth muscle and/or connective tissue present in these preparations since similar results were observed for isolated cardiomyocytes further purified by a Percoll density gradient, to remove non-cardiac cells (Fig. 1A, purified cardiomyocytes; [28]). These data are consistent with recent publications that indicate the presence of mRNA for all 3 RyR subtypes in human heart and vascular muscle cells [29–31].

3.2. Subtype-specific antibodies detect RyR1 in mitochondria isolated from rat and mouse hearts

RT-PCR does not provide information regarding the subcellular location of the three RyR subtypes. Therefore, we used specific antibodies to determine the RyR subtype in SR, intact mitochondria, purified IMM from rat hearts, and isolated heart mitochondria from adult and neonatal mice. Fig. 1B shows representative blots obtained from a concurrent experiment using 4 different RyR antibodies. With an antibody that detects all three RyR subtypes (RyR1–3), we found RyR protein in the SR or the ER enriched microsomes from rat skeletal muscle, heart, and brain (Fig. 1B, RyR1–3, lanes a, b, and c, respectively; $n=8$). This antibody also detected RyR protein in mitochondria and IMM preparations isolated from rat hearts (Fig. 1B, RyR1–3, lanes d and e; $n=13$). The signal in the IMM was stronger relative to that obtained from isolated mitochondria because the RyR protein in purified IMM preparations becomes concentrated without the presence of proteins from the outer mitochondrial membrane and the matrix. Mitochondria isolated from adult mouse hearts also tested positive for RyR protein (Fig. 1B, RyR1–3, lane f; $n=5$), and no RyR protein was detected in mitochondria from neonatal homozygous RyR1 knockout mice (Fig. 1B, RyR1–3, lanes g and h; $n=5$).

As expected, the RyR1-specific antibody, XA 7B6 [32,33], readily detected RyR1 in SR-microsomes from skeletal muscle (Fig. 1B, RyR1, lane a; $n=5$). Interestingly, this antibody also detected RyR protein in mitochondria and IMM vesicles from rat hearts (Fig. 1B, RyR1, lanes d and e; $n=5$). A RyR1-specific signal was also obtained in heart mitochondria from adult mice (Fig. 1B, RyR1, lane f, Fig. 1C, lanes a_1 and a_2; $n=5$) and neonatal control mice (Fig. 1C, lane b_1 and lane f_2; $n=3$), but not from RyR1 knockout mice (Fig. 1B, RyR1, lane g and h, Fig. 1C, lane c_1 and the lanes b_2–e_2; $n=5$). These data indicate that the RyR1 gene encodes the cardiac mRyR and that the lack of detection of RyR1 protein in cardiac mitochondria from RyR1 knockout mice does not arise from the early developmental state.

The monoclonal antibody C3–33 detects RyR2 with high affinity, but has only a very weak affinity for RyR1 [34]. As expected, cardiac SR-containing microsomes tested positive for RyR2 protein using this antibody (Fig. 1B, RyR2, lane b; $n=5$). However, we obtained no RyR2-specific signal with this antibody in any mitochondrial sample obtained from adult rats, adult mice, or neonatal control or RyR1 knockout mice (Fig. 1B, RyR2, lanes d–h; $n\geq 15$). The absence of RyR2-specific immunoreactivity in all cardiac mitochondrial preparations provides strong evidence that RyR2-containing SR fragments do not contaminate the purified mitochondrial preparations. Similarly, the mitochondrial samples also lacked immunoreactivity to a RyR3-specific antibody (Fig. 1B, RyR3, lanes d–h)

that detected RyR3 protein in the SR and ER microsomes from skeletal muscle and brain cytosol, respectively ($n=4$).

In summary, our results obtained by Western blotting with subtype-specific RyR antibodies and the use of RyR1 knockout mice strongly indicate that RyR1 corresponds to the mRyR (heretofore termed as mRyR1) and that mRyR1 is the only RyR-subtype in heart mitochondria. This result is supported by genetic analysis which do not provide evidence for additional RyR subtypes besides the 3 known subtypes [35,36].

3.3. Pharmacological characterization of mRyR1 by ryanodine, caffeine, and AMPPCP

Because ryanodine preferentially binds to the open state of the RyR, the binding of [^{3}H]ryanodine is widely used as an indicator of RyR activation by a variety of modulatory factors (for review, see [26]). [^{3}H]ryanodine binds in a prototypical bell-shaped Ca^{2+} dependence to isolated heart mitochondria. Maximal [^{3}H]ryanodine binding to isolated mitochondria occurs at ~pCa of 4.4 and is completely blocked at pCa 2 (Fig. 2A, close circles; $n=3$; see also [12]). To substantiate the data obtained by Western blot analysis showing that mRyR is RyR1, we compared [^{3}H]ryanodine binding to mitochondria with that to cardiac and skeletal muscle SR microsomes. We found that [^{3}H]ryanodine binding to cardiac microsomes peaks at pCa 3 and is less sensitive to the inhibition by higher concentrations of Ca^{2+} (Fig. 2A, open circles; $n=3$). Consistent with the results obtained by Western blotting, Ca^{2+}-dependent [^{3}H]ryanodine binding to skeletal muscle microsomes is bell-shaped as observed for the binding to isolated mitochondria (Fig. 2A, open rectangles). Both the lower sensitivity of RyR2 to Ca^{2+}-dependent inactivation of [^{3}H]ryanodine binding and the bell-shaped binding curve to skeletal muscle microsomes (Fig. 2A) are consistent with the published literature [37]. The maximal [^{3}H]ryanodine binding to cardiac and skeletal muscle microsomes (per mg protein) was several times higher than that of heart mitochondria, indicating considerably fewer ryanodine binding sites in mitochondria, while the K_d's are virtually identical [12,38].

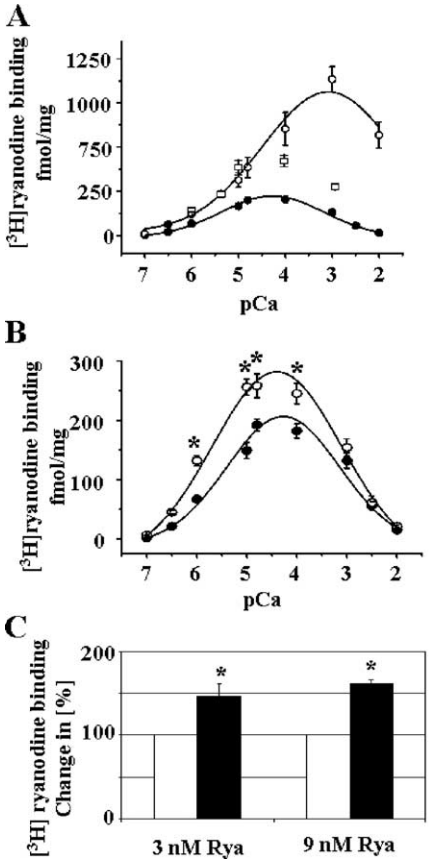

Fig. 2. Modulation of [^{3}H]ryanodine binding to isolated rat heart mitochondria by ryanodine caffeine, and AMPPCP. (A) Ca^{2+} dependency of [^{3}H]ryanodine binding to isolated heart mitochondria (●), cardiac SR (○) and skeletal muscle SR microsomes (□). (B) Ca^{2+} dependency of [^{3}H]ryanodine binding to isolated rat heart mitochondria in absence (●) or presence (○) of 10 mM caffeine. (C) AMPPCP increases [^{3}H]ryanodine binding. Mitochondria were incubated in the absence (white column) or presence (black column) of 2 mM AMPPCP and the indicated concentration of [^{3}H]ryanodine. For both experiments, the binding of [^{3}H]ryanodine in absence of AMPPCP was set to be 100%; data represent the mean of 3 experiments ± S.E. Asterisks (*) indicate statistical significance ($P \leq 0.05$).

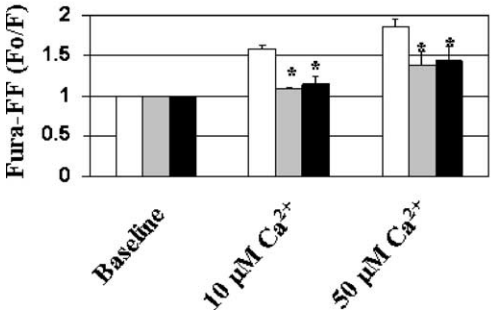

Fig. 3. Ryanodine and dantrolene inhibit mitochondrial Ca^{2+} uptake. Fura-FF-loaded isolated heart mitochondria from rat were challenged with 10 or 50 μM Ca^{2+} and mitochondrial Ca^{2+} uptake was measured (white columns). Preincubating mitochondria for 15 min with 10 μM dantrolene (black columns) or 20 μM ryanodine (gray columns) inhibited Ca^{2+} uptake. The excitation wavelength was 380 nm and the emission wavelength was 510 nm. Under these experimental conditions, mitochondrial Ca^{2+} uptake causes a decrease in the fluorescence (F) signal, which was normalized to the baseline fluorescence (F_o) at the begin of the experiment. Results are expressed as [F_o/F], so that the ratio before the addition of Ca^{2+} is 1 and mitochondrial Ca^{2+} net uptake is reflected as an increase of the ratio. Data represent the average of 4 experiments ± S.E., and asterisks (*) indicate statistical significance ($P<0.01$).

Caffeine is known to increase [^{3}H]ryanodine binding to the skeletal and cardiac SR-RyR in a distinct pattern [15]. Using isolated heart mitochondria maximal [^{3}H]ryanodine binding increased about 30% in the presence of 10 mM caffeine at pCa 4–5 (Fig. 2B, 3–6 experiments per Ca^{2+} concentration; $P \leq 0.05$). This observed increase in [^{3}H]ryanodine binding to isolated heart mitochondria by caffeine is quantitatively similar to that described for RyR1 in the skeletal muscle and is significantly less than that observed for cardiac RyR2, where caffeine causes a much more pronounced increase of [^{3}H]ryanodine binding [15].

The non-hydrolysable ATP-analogue AMPPCP increases Ca^{2+}-stimulated [^{3}H]ryanodine binding to RyR1, but not RyR2 [15,39]. Therefore, heart mitochondria were incubated in the presence of 2 mM AMPPCP and 20 μM Ca^{2+} with 3

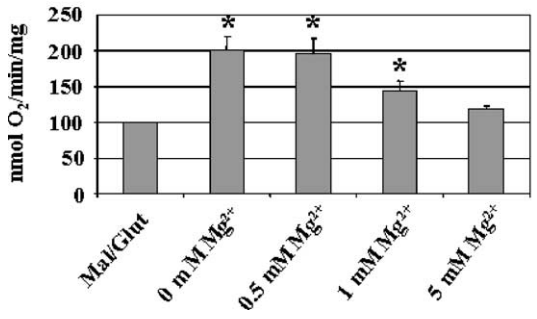

Fig. 4. Ca^{2+} stimulated O_2 consumption in isolated heart mitochondria in the presence of different concentrations of Mg^{2+}. The experimental conditions are described in Methods. Although 1 mM Mg^{2+} lowers the response to Ca^{2+} stimulated O_2 consumption, the stimulating effect of Ca^{2+} still remains significant ($P \leq 0.006$).

or 9 nM [^{3}H]ryanodine. These experimental conditions increased [^{3}H]ryanodine binding to isolated mitochondria up to 61±5.2% (Fig. 2C; $n=5$), and maximal [^{3}H]ryanodine binding in the absence of AMPPCP was set to be 100%. This effect of AMPPCP-increased [^{3}H]ryanodine binding is consistent with the behavior of RyR1.

3.4. Ryanodine inhibits Ca^{2+} stimulated oxygen consumption

An increase in the mitochondrial matrix Ca^{2+} concentration activates the pyruvate-, isocitrate-, and α-ketoglutarate dehydrogenase in the TCA cycle to generate NADH and FADH [4]. The complexes of the electron transport chain then use these substrates for mitochondrial ATP generation by oxidative phosphorylation. To test the role of Ca^{2+} influx via mRyR1 on modulating oxidative phosphorylation, it is essential to expose mitochondria to Ca^{2+} concentrations that preferentially stimulate mRyR1 but not CaUP. Therefore, mitochondrial Ca^{2+} net uptake and the inhibition by ryanodine and dantrolene were directly monitored with the low affinity Ca^{2+} indicator Fura-FF (Fig. 3). The Fura-FF signal, expressed as F_o/F, increased from 1 (baseline) to 1.6±0.04 ($n=4$; $P \leq 0.01$) when extramitochondrial Ca^{2+} concentration was raised to 10 μM. This increase was significantly abolished after pre-incubating mitochondria with ryanodine or dantrolene (1.08±0.017 and 1.14±0.093, respectively; $n=4$). The net uptake of Ca^{2+} at a higher concentration of extramitochondrial Ca^{2+} (50 μM) was inhibited less effectively by ryanodine and dantrolene (Fig. 3), likely due to the activation of other Ca^{2+} uptake mechanisms such as the CaUP. Therefore, we used 10 μM Ca^{2+} to stimulate oxidative phosphorylation.

We measured O_2 consumption in isolated heart mitochondria in the presence of Mg^{2+}, because it improved the state 2 respiration significantly in our experiments. However, Mg^{2+} is known to close the Ca^{2+} channel in the ryanodine receptor [26] and the CaUP [8]. To account for this inhibitory effect of Mg^{2+}, we determined O_2 consumption in the presence of 0, 0.5, 1, and 5 mM Mg^{2+}. Oxygen consumption in the presence of 1 mM Mg^{2+} was only slightly less compared to 0 or 0.5 mM Mg^{2+} (Fig. 4; $n=4$). In the presence of 5 mM Mg^{2+}, O_2 consumption was significantly inhibited.

State 2 respiration in the presence of malate and glutamate was 43.5±7.1 nmol O_2/min/mg mitochondrial protein and increased to 60.5±5.6 nmol O_2/min/mg protein after the addition of 10 μM Ca^{2+} (Table 2; $n=5$; $P \leq 0.05$). However, after pre-incubating isolated heart mitochondria with 20 μM ryanodine, 10 μM Ca^{2+} was not longer effective to stimulate O_2 consumption (50±6.4 nmol/O_2/min/mg protein compared to 48.8±4.8 nmol O_2/min/mg before the addition of Ca^{2+}; $n=5$). Ryanodine itself did not cause the inhibitory effect by interfering with the mitochondrial functionality, because the RCI, an indicator of mitochondrial function, did not change (4.5±1.1 and 4.5±0.8, for control and ryanodine-treated mitochondria, respectively; Table 2; $n=5$). To account for a possible contamination of the mitochondria by Ca^{2+} filled SR vesicles we performed this experiment in the presence of cyclopiazonic acid to empty these vesicles and to inhibit Ca^{2+} uptake into SR vesicles by SERCA. However, the presence of 30 μM cyclopiazonic acid did not change Ca^{2+} stimulated O_2 consumption either in the presence or absence of ryanodine (data not shown).

Addition of 10 μM Ca^{2+} also increased O_2 consumption in heart homogenates of neonatal control mice from 27.0±3.5 nmol O_2/min/mg ($n=5$) to 35.4±3.1 nmol O_2/min/mg (Table 2; $n=4$; $P \leq 0.05$). Similar to isolated heart mitochondria from adult rats, pre-incubation of heart homogenates from neonatal control mice with 20 μM ryanodine abolished Ca^{2+}-stimulated oxidative activity (28.0±3.5 nmol O_2/min/mg and 27.2±1.5 nmol/O_2/min/mg before and after the addition of Ca^{2+}, respectively; $n=4$). Again, the presence of cyclopiazonic acid had no effect on Ca^{2+} stimulated oxidative phosphorylation in neonatal control mice (data not shown).

Table 2
Ca^{2+} stimulated O_2 consumption of isolated mitochondria from rat heart and the tissue homogenate from neonatal control mouse hearts

	0 μM ryanodine			20 μM ryanodine		
	Substr.	Substr.+Ca^{2+}	RCI	Substr.	Substr.+Ca^{2+}	RCI
Adult rat ($n=5$)	43.48±7.09	60.51±5.59	4.5±1.09	48.77±4.84	50.04±6.38	4.5±0.82
Neonatal control mice ($n=5$)	26.97±3.53	35.37±3.13	2.47±0.2	28.02±3.53	27.2±1.49	2.4±0.31
Neonatal RyR1 −/− mice ($n=5$)	36.28±5.53	35.6±8.41	1.12±0.2			

Substr.: oxidative activity in presence of 5 mM malate and 5 mM glutamate. Substr+Ca^{2+}: increase of oxidative activity by 10 μM Ca^{2+}. RCI: respiratory control index; defined in this experiment as the ratio of maximal respiration in presence of 5 mM malate and 5 mM glutamate and 1 mM ADP over substrate-induced (malate and glutamate) respiration. After pre-incubation with 20 μM ryanodine, Ca^{2+} stimulated oxidative activity was inhibited. Values are given as nmol O_2/min/mg protein (except for the RCI)±S.E. and * indicates statistical significance ($P \leq 0.05$).

In heart homogenates obtained from neonatal RyR1 knockout mice, addition of 10 μM Ca^{2+} did not further stimulate mitochondrial oxidative activity, because the substrates malate and glutamate itself caused already maximal O_2 consumption (36.3±5.5 nmol O_2/min/mg and 35.6±8.4 nmol O_2/min/mg in the absence and presence of 10 μM Ca^{2+}, respectively; $n=5$). In these experiments, the addition of Ca^{2+}, ADP, the uncoupler dinitrophenol, or atractyloside, an inhibitor of the adenine nucleotide translocator, did not change the rate of O_2 consumption. However, the very low RCI of RyR1 knockout mice (1.12±0.04 compared to 2.47±0.2 of control mice) indicates that the expression of mRyR1 appears to be essential for the normal respiration of cardiac mitochondria (Table 2).

4. Discussion

The specific aims of this study were to identify the subtype of RyR in mitochondria and to show that Ca^{2+} via mRyR is a critical component for mitochondrial energy production.

4.1. Characterization of the mRyR as RyR1

The data presented here demonstrate that the RyR in cardiac mitochondria exhibits biochemical, pharmacological, and functional properties, remarkably similar to those of RyR1 in the SR of skeletal muscle, and is therefore termed as mRyR1. We used isolated mitochondria from four different resources: adult rats, adult mice, newborn control and newborn RyR1 knockout mice. Dyspedic RyR1 knockout mice contain 2 disrupted alleles for RyR1 resulting in a lethal birth defect [20,21]. To compensate for possible developmental differences between the newborn mice and adult animals, all experiments were repeated with newborn surviving control mice, which were either homozygous (+/+) or heterozygous (+/−) for RyR1. Even though RyR1 knockout mice have no functional RyR1 in the SR, many ultrastructural details of the triadic junctions are still detectable in these mice [20]. However, important differences are that dyspedic muscles lack the regularly spaced array of junctional feet that span the gap between the T-tubule and SR membranes and they also lack the tetradic arrangement of dihydropyridine receptors.

In our experiments, the subtype specific antibody XA7B6 detects RyR1 protein in mitochondria from adult rat or mouse hearts (Fig. 1B). The specificity of this antibody is confirmed by the presence of a RyR1 signal in the skeletal muscle SR but not in the cardiac SR or mitochondria obtained from RyR1 knockout mice (Fig. 1B). In addition, the presence of RyR1 protein in neonatal control mice, which are either homozygous or heterozygous for RyR1, minimizes the possibility that the absence of RyR1 protein in RyR1 knockout mice is due to the developmental stage of the mice. The less pronounced RyR1 signal in newborn mice compared to adult mice can be explained by a lower expression at this early age or the possibility that the majority of the control mice were heterozygous for RyR1. The signal for RyR1 protein obtained from IMM vesicles is stronger than that from isolated mitochondria, indicating a higher concentration of RyR1 protein in the IMM compared to the intact mitochondria. Although we obtained the mRNA message for RyR3 in heart tissue and isolated cardiomyocytes, we could not detect RyR3 protein in the tested cardiac subfractions (Fig. 1B). It is likely that the expression level of RyR3 is very low and thus beyond the detection limit of Western blot analysis.

Even though genetic analysis provides no evidence for additional RyR-subtypes besides the 3 known subtypes [35,36], the here presented results cannot exclude the possibility that mRyR1 is a splice variant of RyR1. Indeed, it has been shown that the used RyR1 specific antibody XA 7B6 still detects a 172-kDa N-terminal cleavage product of RyR1 [40]. In addition, splice variants of RyR2 and RyR3 have been identified [41,42].

The pharmacological profile of modulation of [^{3}H] ryanodine binding to isolated mitochondria by Ca^{2+}, caffeine, and AMPPCP provides further evidence that mRyR is RyR1. The Ca^{2+}-dependent binding of [^{3}H]ryanodine to cardiac mitochondria is biphasic (Fig. 2A) and resembles the characteristics of [^{3}H]ryanodine binding to RyR1 in the SR of skeletal muscle [39]. Inhibition of [^{3}H]ryanodine binding to RyR1 has been described for pCa ≥ 4 (for review, see [26]). In contrast, Ca^{2+} dependent inhibition of [^{3}H]ryanodine binding to the cardiac RyR2-subtype requires much higher concentrations of Ca^{2+} (Fig. 2A) [39]. Furthermore, the characteristics of caffeine and AMPPCP modulation coincide with that of RyR1 not of RyR2 (Fig. 2B and C, [15,37]). Finally, dantrolene, which inhibits more selectively the Ca^{2+} channel of RyR1 [43], blocks mitochondrial Ca^{2+} net uptake effectively and thus, adds functional evidence that mRyR is RyR1 (Fig. 3).

4.2. Functional implication of differential location of RyR1 and RyR2 in cardiac muscle cells

Our data obtained by Western Blot analysis of subcellular fractions indicate that in the heart RyR2 is localized in the SR, while RyR1 is localized in mitochondria. One reason for this differential localization of RyRs in cardiac muscle cells is that they serve for different functional roles. In cardiac muscle cells, Ca^{2+} influx through voltage gated Ca^{2+} channels activate RyR2 channels, resulting in Ca^{2+} induced Ca^{2+} release from the SR. The Ca^{2+}-dependency of ryanodine binding implies that a micro-domain of high Ca^{2+}, near SR−mitochondria junction, does not inactivate RyR2 significantly during excitation−contraction coupling, so that a large amount of Ca^{2+} can be released from the SR to trigger muscle contraction. On the contrary, the bell-shaped pCa-dependence of ryanodine binding suggests that mRyR1 becomes activated as soon as Ca^{2+} is released from the SR and will be maximally activated at Ca^{2+} concentrations of about 10 to 40 μM. Further increases in the local Ca^{2+} concentration lead to inactivation of mRyR1 to prevent mitochondrial Ca^{2+} overload and opening of permeability transition pore.

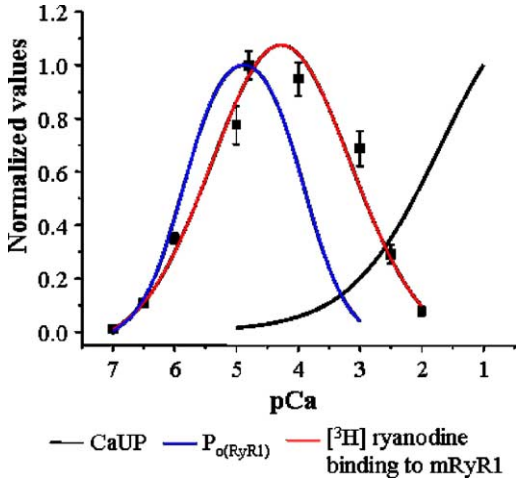

Fig. 5. Simulation of Ca^{2+} sensitivity of mRyR1 and CaUP. In this graph the normalized Ca^{2+} dependent CaUP current (I_{CaUP}, black line) was simulated according to [10]. The normalized open probability of RyR1 ($P_{o(RyR1)}$, blue line) was simulated according to [50]. The red line represents our [^{3}H]ryanodine binding data (filled squares, red line) from isolated rat heart mitochondria. The simulation shows that the open probability of RyR1 and the Ca^{2+} dependency of [^{3}H]ryanodine binding to isolated heart mitochondria appear not significantly different.

It has been recognized for some time that Mg^{2+} has an inhibitory effect on the RyRs [44,45] and one would expect that Mg^{2+} inhibits mRyR1 under physiological conditions [46]. However, the concentration of Mg^{2+} to inhibit RyR2 by 50% is a few mM, which is approximately 10 times higher than that for inhibiting RyR1 (~0.3 mM). Mg^{2+} inhibits the non-phosphorylated RyR. In the presence of ATP or other adenine nucleotides, Ca^{2+} permeability through RyR is increased even in the presence of physiological concentrations of Mg^{2+} [38]. In addition, it is possible that the formation of Mg-ATP in the intermembrane space keeps the free concentration of Mg^{2+} locally low enough to prevent a complete inhibition of mRyR1. Furthermore, the presence of Mg-ATP is essential for the function of a number of mitochondrial kinases or the mitochondrial K_{ATP}-channel.

Functionally, the RyR1 in the skeletal muscle is coupled to the activity of voltage activated, dihydropyridine-sensitive Ca^{2+} channels [37]. Opening of this channel via depolarization transmits the activating signal to RyR1. An interesting hypothesis for mRyR1 is that Ca^{2+} influx through VDAC could transmit the activating signal to mRyR1. It has been shown that VDAC has the ability to regulate Ca^{2+} transport across the outer mitochondrial membrane [47]. The selectivity of VDAC for cations or anions in bilayer experiments depends on the applied voltage [48] and could provide in vivo a model how VDAC channels regulate mRyR1. This mechanism would allow a regulated Ca^{2+} flow across the outer mitochondrial membrane as well as Ca^{2+} influx into the mitochondrial matrix.

4.3. Simulation of Ca^{2+} dependency of mRyR1 versus CaUP

Despite the unknown molecular identity, the functional properties of CaUP are well established (for reviews see [8,49]). In general, the results show that the relationship between the initial rates of Ca^{2+} uptake by CaUP and the extra mitochondrial Ca^{2+} concentration is sigmoidal, assuming a Hill coefficient of 2 and a half maximal transport velocity varying

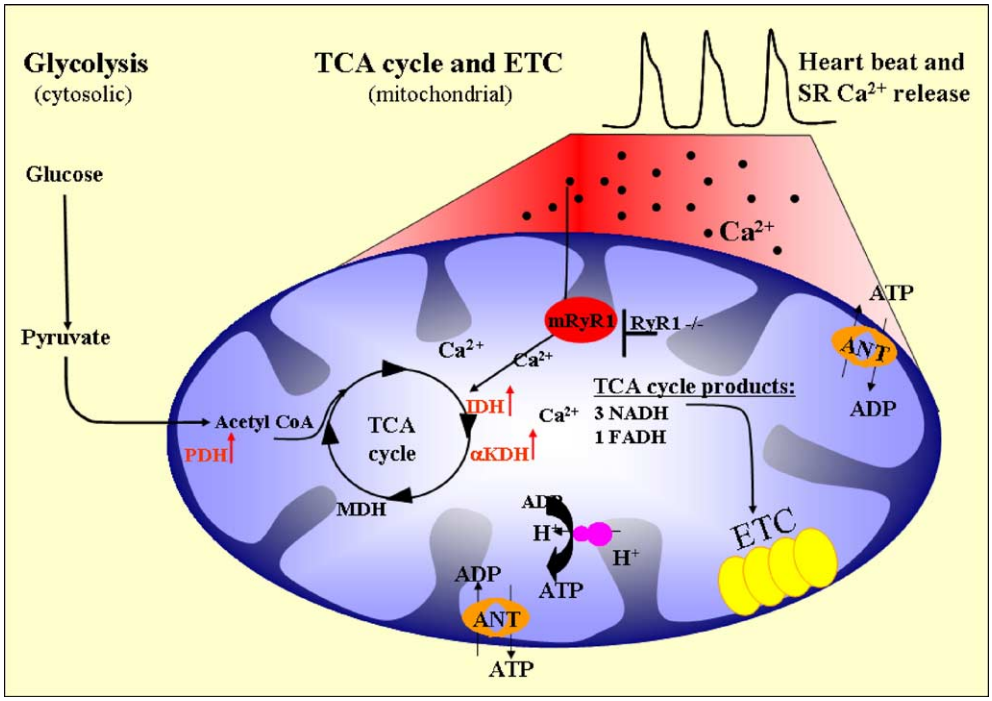

Fig. 6. The mRyR1 as a transducer of excitation–metabolism coupling. With each heart beat Ca^{2+} is released from the SR into the cytosol (indicated by the red area around the mitochondria). Hypothetically, mitochondria in close proximity to the SR could respond with fast mitochondrial Ca^{2+} uptake mediated by mRyR1 to activate several dehydrogenases associated with the TCA cycle (highlighted in red) and subsequent oxidative phosphorylation. PDH, pyruvate dehydrogenase; IDH, isocitrate dehydrogenase; KDH, α-ketoglutarate dehydrogenase; MDH malate dehydrogenase; ETC electron transport chain.

between 1 and 189 μM [49]. This long established view of mitochondrial Ca^{2+} uptake by the CaUP has been challenged recently by a study using patch-clamp to record CaUP currents in mitoplasts isolated from COS-7 cell [10]. In these experiments, half-maximal saturation of the CaUP was achieved at approximately 20 mM Ca^{2+} and reached saturation at 105 mM [10]. Plotting the normalized currents of CaUP and RyR1 as a function of Ca^{2+} concentration using the assumptions discussed in [10] and [50], respectively, shows that the open probability of RyR1 peaks in the presence of 10–30 μM Ca^{2+} (Fig. 5, blue trace), while the CaUP is fully activated at much higher concentrations of Ca^{2+} (Fig. 5, black trace). Our data of [^{3}H]ryanodine binding to isolated mitochondria at different concentration of Ca^{2+} indicate that mRyR1 becomes activated at low concentrations of Ca^{2+} and inactivated by higher Ca^{2+} concentration like RyR1 (Fig. 5, red trace). This analysis suggests that the CaUP with its low affinity and high capacity for mitochondrial Ca^{2+} uptake is better suited for reducing a possible cytosolic Ca^{2+} overload to prevent necrotic or apoptotic cell death [8].

4.4. Ca^{2+} stimulated O_2 consumption is inhibited by ryanodine

Our experiments show that Ca^{2+} uptake via mRyR1 stimulates O_2 consumption when the extramitochondrial Ca^{2+} concentration was raised to 10 μM. This process is inhibited by ryanodine. Interestingly, at 50 μM extra-mitochondrial Ca^{2+} concentration, the inhibitory effects by ryanodine or dantrolene became smaller. It is likely that the mitochondrial CaUP becomes activated at this concentration of Ca^{2+}, consistent with the simulated Ca^{2+} dependencies shown in Fig. 5. Ca^{2+} stimulated O_2 consumption was not measurable in tissue homogenates from RyR1 knockout mice, because the addition of substrates alone increased already O_2 consumption to a level not distinguishable from maximal respiration induced by the addition of dinitrophenol. The rate of O_2 consumption did also not change upon the addition of ADP (to stimulate maximal respiration) or atractyloside, an inhibitor of the adenine nucleotide translocase, indicating the loss of mitochondrial function in RyR1 knockout mice.

The close proximity between SR and mitochondria allows the formation of discrete micro-domains with high Ca^{2+} concentration, sufficient to activate rapid mitochondrial Ca^{2+} uptake mechanisms [51,52]. However, the low affinity of the CaUP for Ca^{2+} ($K_d \geq 50$ μM) and the velocity of Ca^{2+} uptake [8] make this Ca^{2+} channel a poor candidate to regulate Ca^{2+}-induced ATP generation on a beat-to-beat basis. In contrast, the K_m of the high affinity binding site of RyR1/mRyR1 for Ca^{2+} activation is about 1μM [14,53], and sufficient to connect cardiac excitation–contraction coupling with mitochondrial energy metabolism during physiological Ca^{2+} oscillations. Together, these results would support a concept of "excitation–metabolism coupling" (Fig. 6). In this scheme, cytosolic Ca^{2+} oscillations during heartbeats could trigger mitochondrial Ca^{2+} uptake via the mRyR1 and subsequently activate Ca^{2+} regulated dehydrogenases in the TCA cycle. NADH and FADH, the products of the TCA cycle, would then increase ATP generation by entering the electron transport chain and stimulation of oxidative phosphorylation.

In conclusion, mRyR1 may function as a transducer of myoplasmic Ca^{2+} signals into the mitochondria to regulate energy generation. Since cellular Ca^{2+} homeostasis, ATP generation, and reactive oxygen species production are crucial in maintaining life, dysfunction of mRyR may be critical in the etiology of diseases such as skeletal and cardiac myopathy, ischemia–reperfusion injury, central core disease and neurodegenerative diseases [54].

Acknowledgments

We thank current and past members of the Sheu laboratory, Beth Altschaffl, Drs. Paul Brooks, Howard Federoff, Yisang Yoon, Hector Valdivia and David Yule for helpful comments, critical reading, and discussions on the manuscript. We also thank Dr. Paul Allen for providing us access to the RyR1 knockout mice used in this study. This work was supported by NIH grants HL-33333 and NS-37710 (SSS), AR-44657 (RTD), AHA grants 0050839T (SSS) and 0335425T (GB).

References

[1] D.F. Babcock, J. Herrington, P.C. Goodwin, Y.B. Park, B. Hille, Mitochondrial participation in the intracellular Ca2+ network, J. Cell Biol. 136 (1997) 833–844.
[2] M.J. Berridge, P. Lipp, M.D. Bootman, The versatility and universality of calcium signalling, Nat. Rev., Mol. Cell. Biol. 1 (2000) 11–21.
[3] G. Hajnoczky, L.D. Robb-Gaspers, M.B. Seitz, A.P. Thomas, Decoding of cytosolic calcium oscillations in the mitochondria, Cell 82 (1995) 415–424.
[4] R.G. Hansford, Physiological role of mitochondrial Ca2+ transport, J. Bioenerg. Biomembr. 26 (1994) 495–508.
[5] D.C. Wallace, Mitochondrial defects in cardiomyopathy and neuromuscular disease, Am. Heart J. 139 (2000) S70–S85.
[6] K.D. Gerbitz, K. Gempel, D. Brdiczka, Mitochondria and diabetes. Genetic, biochemical, and clinical implications of the cellular energy circuit, Diabetes 45 (1996) 113–126.
[7] D.G. Nicholls, S.L. Budd, Mitochondria and neuronal survival, Physiol. Rev. 80 (2000) 315–360.
[8] T.E. Gunter, K.K. Gunter, S.S. Sheu, C.E. Gavin, Mitochondrial calcium transport: physiological and pathological relevance, Am. J. Physiol. 267 (1994) C313–C339.
[9] K.W. Kinnally, M.L. Campo, H. Tedeschi, Mitochondrial channel activity studied by patch-clamping mitoplasts, J. Bioenerg. Biomembr. 21 (1989) 497–506.
[10] Y. Kirichok, G. Krapivinsky, D.E. Clapham, The mitochondrial calcium uniporter is a highly selective ion channel, Nature 427 (2004) 360–364.
[11] J.E. Kokoszka, K.G. Waymire, S.E. Levy, J.E. Sligh, J. Cai, D.P. Jones, G.R. MacGregor, D.C. Wallace, The ADP/ATP translocator is not essential for the mitochondrial permeability transition pore, Nature 427 (2004) 461–465.
[12] G. Beutner, V.K. Sharma, D.R. Giovannucci, D.I. Yule, S.S. Sheu, Identification of a ryanodine receptor in rat heart mitochondria, J. Biol. Chem. 276 (2001) 21482–21488.
[13] S.R. Holmberg, A.J. Williams, Patterns of interaction between anthraquinone drugs and the calcium- release channel from cardiac sarcoplasmic reticulum, Circ. Res. 67 (1990) 272–283.
[14] I.N. Pessah, A.L. Waterhouse, J.E. Casida, The calcium–ryanodine receptor complex of skeletal and cardiac muscle, Biochem. Biophys. Res. Commun. 128 (1985) 449–456.

[15] I. Zimanyi, I.N. Pessah, Comparison of [3H]ryanodine receptors and Ca++ release from rat cardiac and rabbit skeletal muscle sarcoplasmic reticulum, J. Pharmacol. Exp. Ther. 256 (1991) 938–946.
[16] R.S. Balaban, Cardiac energy metabolism homeostasis: role of cytosolic calcium, J. Mol. Cell. Cardiol. 34 (2002) 1259–1271.
[17] S. Rehncrona, L. Mela, B.K. Siesjo, Recovery of brain mitochondrial function in the rat after complete and incomplete cerebral ischemia, Stroke 10 (1979) 437–446.
[18] A. Saito, S. Seiler, A. Chu, S. Fleischer, Preparation and morphology of sarcoplasmic reticulum terminal cisternae from rabbit skeletal muscle, J. Cell Biol. 99 (1984) 875–885.
[19] K. Ohlendieck, I. Riesinger, V. Adams, J. Krause, D. Brdiczka, Enrichment and biochemical characterization of boundary membrane contact sites from rat-liver mitochondria, Biochim. Biophys. Acta 860 (1986) 672–689.
[20] E.D. Buck, H.T. Nguyen, I.N. Pessah, P.D. Allen, Dyspedic mouse skeletal muscle expresses major elements of the triadic junction but lacks detectable ryanodine receptor protein and function, J. Biol. Chem. 272 (1997) 7360–7367.
[21] H. Takeshima, M. Iino, H. Takekura, M. Nishi, J. Kuno, O. Minowa, H. Takano, T. Noda, Excitation–contraction uncoupling and muscular degeneration in mice lacking functional skeletal muscle ryanodine-receptor gene, Nature 369 (1994) 556–559.
[22] A. Fabiato, F. Fabiato, Calculator programs for computing the composition of the solutions containing multiple metals and ligands used for experiments in skinned muscle cells, J. Physiol. (Paris) 75 (1979) 463–505.
[23] R.S. Balaban, S. Bose, S.A. French, P.R. Territo, Role of calcium in metabolic signaling between cardiac sarcoplasmic reticulum and mitochondria in vitro, Am. J. Physiol.: Cell Physiol. 284 (2003) C285–C293.
[24] G. Villani, G. Attardi, In vivo measurements of respiration control by cytochrome *c* oxidase and in situ analysis of oxidative phosphorylation, Methods Cell Biol. 65 (2001) 119–131.
[25] C. Franzini-Armstrong, F. Protasi, Ryanodine receptors of striated muscles: a complex channel capable of multiple interactions, Physiol. Rev. 77 (1997) 699–729.
[26] V. Shoshan-Barmatz, R.H. Ashley, The structure, function, and cellular regulation of ryanodine-sensitive Ca2+ release channels, Int. Rev. Cytol. 183 (1998) 185–270.
[27] P. Tarroni, D. Rossi, A. Conti, V. Sorrentino, Expression of the ryanodine receptor type 3 calcium release channel during development and differentiation of mammalian skeletal muscle cells, J. Biol. Chem. 272 (1997) 19808–19813.
[28] R.K. Gupta, B.A. Wittenberg, 19F nuclear magnetic resonance studies of free calcium in heart cells, Biophys. J. 65 (1993) 2547–2558.
[29] F. Coussin, N. Macrez, J.L. Morel, J. Mironneau, Requirement of ryanodine receptor subtypes 1 and 2 for Ca(2+)-induced Ca(2+) release in vascular myocytes, J. Biol. Chem. 275 (2000) 9596–9603.
[30] G. Munch, B. Bolck, A. Sugaru, R.H. Schwinger, Isoform expression of the sarcoplasmic reticulum Ca2+ release channel (ryanodine channel) in human myocardium, J. Mol. Med. 78 (2000) 352–360.
[31] C.B. Neylon, S.M. Richards, M.A. Larsen, A. Agrotis, A. Bobik, Multiple types of ryanodine receptor/Ca2+ release channels are expressed in vascular smooth muscle, Biochem. Biophys. Res. Commun. 215 (1995) 814–821.
[32] A.H. Sharp, P.S. McPherson, T.M. Dawson, C. Aoki, K.P. Campbell, S.H. Snyder, Differential immunohistochemical localization of inositol 1,4,5-trisphosphate-and ryanodine-sensitive Ca2+ release channels in rat brain, J. Neurosci. 13 (1993) 3051–3063.
[33] K.P. Campbell, C.M. Knudson, T. Imagawa, A.T. Leung, J.L. Sutko, S.D. Kahl, C.R. Raab, L. Madson, Identification and characterization of the high affinity [3H]ryanodine receptor of the junctional sarcoplasmic reticulum Ca2+ release channel, J. Biol. Chem. 262 (1987) 6460–6463.
[34] F.A. Lai, Q.Y. Liu, L. Xu, A. el-Hashem, N.R. Kramarcy, R. Sealock, G. Meissner, Amphibian ryanodine receptor isoforms are related to those of mammalian skeletal or cardiac muscle, Am. J. Physiol. 263 (1992) C365–C372.
[35] M. Fill, J.A. Copello, Ryanodine receptor calcium release channels, Physiol. Rev. 82 (2002) 893–922.
[36] D. Rossi, V. Sorrentino, Molecular genetics of ryanodine receptors Ca(2+)-release channels, Cell Calcium 32 (2002) 307–319.
[37] L. Xu, A. Tripathy, D.A. Pasek, G. Meissner, Potential for pharmacology of ryanodine receptor/calcium release channels, Ann. N. Y. Acad. Sci. 853 (1998) 130–148.
[38] G. Meissner, E. Darling, J. Eveleth, Kinetics of rapid Ca2+ release by sarcoplasmic reticulum. Effects of Ca2+, Mg2+, and adenine nucleotides, Biochemistry 25 (1986) 236–244.
[39] L. Xu, A. Tripathy, D.A. Pasek, G. Meissner, Ruthenium red modifies the cardiac and skeletal muscle Ca(2+) release channels (ryanodine receptors) by multiple mechanisms, J. Biol. Chem. 274 (1999) 32680–32691.
[40] K. Paul-Pletzer, T. Yamamoto, M.B. Bhat, J. Ma, N. Ikemoto, L.S. Jimenez, H. Morimoto, P.G. Williams, J. Parness, Identification of a dantrolene-binding sequence on the skeletal muscle ryanodine receptor, J. Biol. Chem. 277 (2002) 34918–34923.
[41] W. Chiang, C.P. Allison, J.E. Linz, G.M. Strasburg, Identification of two alphaRYR alleles and characterization of alphaRYR transcript variants in turkey skeletal muscle, Gene 330 (2004) 177–184.
[42] D. Jiang, B. Xiao, X. Li, S.R. Chen, Smooth muscle tissues express a major dominant negative splice variant of the type 3 Ca2+ release channel (ryanodine receptor), J. Biol. Chem. 278 (2003) 4763–4769.
[43] F. Zhao, P. Li, S.R. Chen, C.F. Louis, B.R. Fruen, Dantrolene inhibition of ryanodine receptor Ca2+ release channels. Molecular mechanism and isoform selectivity, J. Biol. Chem. 276 (2001) 13810–13816.
[44] I.N. Pessah, R.A. Stambuk, J.E. Casida, Ca2+-activated ryanodine binding: mechanisms of sensitivity and intensity modulation by Mg2+, caffeine, and adenine nucleotides, Mol. Pharmacol. 31 (1987) 232–238.
[45] J. Hain, H. Onoue, M. Mayrleitner, S. Fleischer, H. Schindler, Phosphorylation modulates the function of the calcium release channel of sarcoplasmic reticulum from cardiac muscle, J. Biol. Chem. 270 (1995) 2074–2081.
[46] L. Garfinkel, R.A. Altschuld, D. Garfinkel, Magnesium in cardiac energy metabolism, J. Mol. Cell. Cardiol. 18 (1986) 1003–1013.
[47] D. Gincel, H. Zaid, V. Shoshan-Barmatz, Calcium binding and translocation by the voltage-dependent anion channel: a possible regulatory mechanism in mitochondrial function, Biochem. J. 358 (2001) 147–155.
[48] R. Benz, M. Kottke, D. Brdiczka, The cationically selective state of the mitochondrial outer membrane pore: a study with intact mitochondria and reconstituted mitochondrial porin, Biochim. Biophys. Acta 1022 (1990) 311–318.
[49] T.E. Gunter, D.R. Pfeiffer, Mechanisms by which mitochondria transport calcium, Am. J. Physiol. 258 (1990) C755–C786.
[50] J.J. Marengo, C. Hidalgo, R. Bull, Sulfhydryl oxidation modifies the calcium dependence of ryanodine-sensitive calcium channels of excitable cells, Biophys. J. 74 (1998) 1263–1277.
[51] V. Ramesh, V.K. Sharma, S.S. Sheu, C. Franzini-Armstrong, Structural proximity of mitochondria to calcium release units in rat ventricular myocardium may suggest a role in Ca2+ sequestration, Ann. N. Y. Acad. Sci. 853 (1998) 341–344.
[52] R. Rizzuto, M. Brini, M. Murgia, T. Pozzan, Microdomains with high Ca2+ close to IP3-sensitive channels that are sensed by neighboring mitochondria, Science 262 (1993) 744–747.
[53] M. Michalak, P. Dupraz, V. Shoshan-Barmatz, Ryanodine binding to sarcoplasmic reticulum membrane; comparison between cardiac and skeletal muscle, Biochim. Biophys. Acta 939 (1988) 587–594.
[54] P.S. Brookes, Y. Yoon, J.L. Robotham, M.W. Anders, S.S. Sheu, Calcium, ATP, and ROS: a mitochondrial love–hate triangle, Am. J. Physiol.: Cell Physiol. 287 (2004) C817–C833.
[55] X. Zhang, J. Wen, K.R. Bidasee, H.R. Besch Jr., R.J. Wojcikiewicz, B. Lee, R.P. Rubin, Ryanodine and inositol trisphosphate receptors are differentially distributed and expressed in rat parotid gland, Biochem. J. 340 (1999) 519–527.